

A simple kriging technique for characterising geotechnical zones of a Zimbabwean Great Dyke deposit

T. Zvarivadza

*Luleå University of Technology, Luleå, Sweden
University of Johannesburg, Johannesburg, South Africa
Tawanda.Zvarivadza@ltu.se; Tawanda.Zvarivadza@vimbogroup.com*

H. Grobler

University of Johannesburg, Johannesburg, South Africa

M. Onifade

Federation University Australia, Ballarat, Victoria 3350, Australia

Abstract

The Great Dyke of Zimbabwe hosts extensive platinum resources, making Zimbabwe the third-largest supplier of platinum in the world. This mineral wealth renders the Dyke economically significant not only to Zimbabwe but also to the global market. To enhance the extraction and ensure the safety of mining operations, a comprehensive drilling campaign comprising 104 drill boreholes was conducted at the studied deposit to geotechnically characterise the rockmass. Given the borehole spacing of over 50 m, there was a critical need to accurately estimate the rockmass quality between drill holes for effective geotechnical input into pillar design, support design, and numerical models. The simple kriging technique was employed to address this challenge, providing reliable estimates of rockmass quality as confirmed by a rigorous cross-validation exercise. Simple kriging offers a significant advantage over traditional empirical methods. Unlike empirical methods, which can be limited by their reliance on direct measurements and assumptions about rockmass behaviour, simple kriging utilises spatial statistics to interpolate and predict rockmass properties with greater precision. This geostatistical method incorporates both the known data points and the spatial correlation between them, leading to more accurate and reliable predictions of rockmass quality. The application of simple kriging facilitated the delineation of distinct geotechnical zones within the deposit. This zoning is crucial for future geotechnical assessments and designs, allowing for a tailored approach to the varying conditions across the deposit. As a result, the delineation of geotechnical zones supports the development of robust pillar designs, enhancing mine safety and sustainability on the Great Dyke. This approach not only ensures the structural integrity of mining operations but also optimises the resource extraction process, ultimately contributing to the long-term economic viability and safety of the mining activities.

Keywords

Great Dyke of Zimbabwe, hardrock platinum mining, geotechnical characterisation, simple kriging, pillar design, mine safety and sustainability



1 Introduction

The 3 km to 10 km wide Great Dyke of Zimbabwe is a significant geological feature extending over 550 km in length, hosting extensive platinum group metal (PGM) resources. As the third-largest supplier of platinum in the world, the mining sector of Zimbabwe plays a crucial role in the global market. Efficient extraction and ensuring the safety of mining operations require a detailed understanding of the geotechnical characteristics of the rockmass within the Dyke. A comprehensive drilling campaign comprising 104 drill boreholes was conducted at the studied deposit to geotechnically characterise the rockmass. However, the borehole spacing of over 50 m presents challenges in accurately estimating the rockmass quality between drill holes. Traditional empirical methods may not suffice due to their limitations in spatial interpolation and reliance on assumptions about rockmass behaviour. As a result, advanced geostatistical methods like simple kriging become essential tools for reliable estimation and characterisation. This paper presents the application of the simple kriging technique to estimate the rockmass quality between boreholes and delineate distinct geotechnical zones within the deposit. The methodology incorporates spatial statistics to interpolate and predict rockmass properties with greater precision, facilitating tailored geotechnical assessments and designs for mining operations on the Great Dyke. Figure 1 presents (a) the location of the Great Dyke and its millions of tonnes of platinum resources as well as (b) its cross-sectional view.

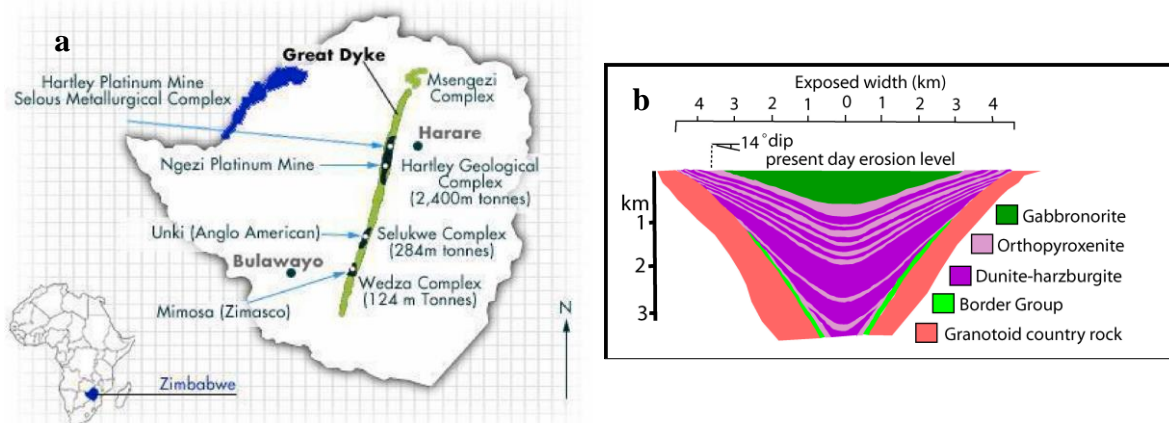


Fig. 1 a) The Great Dyke of Zimbabwe and its platinum resources (Siachingoma et al, 2023). b) The Great Dyke of Zimbabwe Cross-sectional view (Chaumba, 2017 citing Wilson and Prendergast, 1989)

2 Methodology

2.1 Data collection and preparation

The dataset comprises geotechnical parameters obtained from extensive logging of 104 drill boreholes spread across the deposit. Figures 2a (showing a shear zone) and 2b (showing a fracture zone) show example drill core from the study area indicating variation of rockmass quality and structures encountered in the deposit. Table 1 is one of the 104 drill borehole core logs showing various aspects characterised at the study site, these include; rock type and composition; Total Core Recovery (TCR), Solid Core Recovery (SCR), and Rock Quality Designation (RQD); fracturing and joint characteristics; brittle structure properties and alteration zones; water presence and infill types; intact rock strength and fracture frequency etc. The logging nomenclature is given under Table 1b. The logged data was used to determine Rock Mass Rating (RMR) of different portions of the deposit. The spatial coordinates (x_i , y_i) and the corresponding RMR characterisation $Z(x_i)$ form the basis for the spatial analysis presented in this paper.



Fig. 2 Example drill core from the study area indicating variation of rockmass quality and structures. a) shear zone. b) fracture zone

Table 1a Example Log 1 – Quick log per run

From (m)	To (m)	Rock Type	TCR (m)	SCR	RQD L>100mm	Photo Number	Comments
158.32	161.32	Anorthositic norite	3	3	3	BO40-1	OCJs @ 158.78, 160.14, RIR
161.32	162.52	Anorthositic norite	1.2	0.1	0.1	BO40-1	Fr btwn 161.32 & 161.65, Fr btwn 161.74 & 162.52, RIR
162.52	163.37	Anorthositic norite & Websterite @ 162.97	0.85	0.42	0.42	BO40-1	F btwn 162.52 & 162.95, RIR
163.37	164.32	Websterite	0.95	0.95	0.95	BO40-1,2	OCJs @ 163.37, 163.56, 163.83, 164.08, RIR
164.32	165.84	Websterite	1.52	1.52	1.52	BO40-2	OCJs @ 165.08, 165.38, 165.67, RIR
165.84	167.32	Websterite	1.48	1.48	1.48	BO40-2	OCJs @ 166.10, 166.34, 166.52, RIR
167.32	169.29	Websterite	1.97	1.97	1.63	BO40-2	F btwn 167.95 & 168.29, OCJs @ 168.75, 169.29, RIR
169.29	170.32	Websterite	1.03	1.03	1.03	BO40-2	OCJs @ 169.73, 170.11, 170.26, RIR
170.32	171.23	Websterite	0.91	0.91	0.32	BO40-2,3	F btwn 170.32 & 170.78, F btwn 171.10 & 171.23, RIR
171.23	173.32	Websterite & Bronzite @ 172.12	2.09	2.09	2.09	BO40-3	OCJs @ 171.39, 171.53, 171.77, 172.25, 172.84, 173.03, RIR
173.32	175.34	Bronzite	2.02	1.85	1.76	BO40-3	F btwn 173.79 & 173.88, FZ btwn 174.49 & 174.66, OCJ @ 174.77
175.34	176.32	Bronzite	0.98	0.98	0.98	BO40-3	OCJs @ 175.70, 176.02, RIR
176.32	178.14	Bronzite	1.82	1.5	1.5	BO40-3	SZ btwn 176.38 & 176.70, OCJs @ 177.28, 177.43, 177.91

Table 1b Example Log 2 – Major Structures

Distance or Interval		Structure Type		Typical Orientation	Brittle Structure Properties			Water Staining	Description
From (m)	To (m)	Code	Class	Alpha	Micro-scale Geometry	Infill	Alteration		
158.32	158.78	J	2	45	8	SP	1	√	1OCJ, faulted with displacement, RIR
158.78	160.14	J	2	45	8	SP	1	√	1OCJ, faulted with displacement, RIR
160.14	161.32	–	–	–	–	–	–	–	Wholly intact rock
161.32	165.65	Fr	3	–	–	SP	1	√	Weakened by alteration
165.65	161.74	–	–	–	–	–	–	–	Wholly intact rock
161.74	162.52	Fr	3	–	–	CHL & SP	3	√	Rockmass weakened by strong fracturing
162.52	162.95	F	2	85	5	SP	1	√	faulted with displacement, RIR
162.95	163.37	J	3	45	4	SP	1	√	1OCJ, faulted with displacement, RIR
163.37	163.56	J	2	20	1	SP	1	√	1OCJ, faulted with displacement, RIR
163.56	163.83	–	–	–	–	–	–	–	Wholly intact rock
163.83	164.08	F	2	45	8	SP	1	√	2OCJs, faulted with displacement, RIR
164.08	165.08	J	2	55	8	SP	1	√	1OCJ, faulted with displacement, RIR
165.08	165.38	J	2	30	8	SP	1	√	1OCJ, faulted with displacement, RIR
165.38	165.67	J	2	65	8	SP	1	√	1OCJ, faulted with displacement, RIR
165.67	166.1	J	2	38	1	SP	1	√	1OCJ, faulted with displacement, RIR
166.1	166.52	J	2	45	8	SP	1	√	2OCJs, faulted with displacement, RIR
166.52	168.29	F	2	88	–	SP	3	√	Multiple joints, faulted with displacement, RIR
168.29	168.75	J	2	35	8	SP	1	√	1OCJ, faulted with displacement, RIR
168.75	169.29	J	2	35	8	SP	1	√	1OCJ, faulted with displacement, RIR
169.29	169.73	J	2	45	8	SP	1	√	1OCJ, faulted with displacement, RIR
169.73	170.11	J	2	87	4	SP	1	√	1OCJ, Weakened by alteration
170.11	170.26	J	2	34	8	SP	1	√	1OCJ, faulted with displacement, RIR
170.26	170.32	–	–	–	–	–	–	–	Wholly intact rock
170.32	171.1	F	2	45	8	SP	1	√	3OCJs, faulted with displacement, RIR
171.1	171.23	F	2	45	8	SP	1	√	3OCJs, faulted with displacement, RIR
171.23	173.03	F	2	45	5	SP	1	√	6OCJs, faulted with displacement, RIR
173.03	173.79	–	–	–	–	–	–	–	Wholly intact rock
173.79	174.49	F	2	55	8	SP	1	√	3OCJs, Weakened by alteration, RIR
174.49	174.66	Fr	3	–	–	SP	3	√	Rockmass weakened by strong fracturing
174.66	176.38	F	2	55	8	SP	1	√	3OCJs, faulted with displacement, RIR
176.38	177.28	SZ	5	–	–	SP	3	√	Core completely altered to residual soil
177.28	177.91	F	2	45	8	SP	1	√	3OCJs, faulted with displacement, RIR

Structure Code: Shear Zone (SZ); Fracture Zone (FZ); Fault (F); Fracture (Fr); Joint (J); Striation lineation (L); Fold Axis (FA); Vein (V); Dyke (D).

Structure Class: Strongly sheared (cataclasite/mylonite), or brecciated (1); Clearly faulted with displacement or striations (2); The rockmass is weakened by alteration or strong fracturing, a nearby major structure is likely (3); The core is completely broken because of poor core recovery. Possibly structure related (4); Core is strongly or completely altered/weathered to residual soil/mud (5). **Fill Type:** Q – Quartz; G – Gouge; C – Calcite; M – Magnesium; FE – Iron oxide; H – Haematite; CL – Clay; S – Sulphide; B – Breccia; O – Other. **Wall Alteration:** 1 - wall=rock hardness; 2 - wall>rock hardness; 3 - wall<rock hardness.

Micro/Small Scale Joint Expression: Rough/Stepped/Irregular - 1; Smooth Stepped - 2; Slickensided Stepped - 3; Rough Undulating - 4; Smooth Undulating - 5; Slickensided Undulating - 6; Rough Planar - 7; Smooth Planar - 8; Polished - 9. **Other Descriptions:** OCJ - Open Cemented Joints; RIR - Rest Intact Rock; Btw – Between; Tot – Total; Nat – Natural; Fol – Foliation; S1 – Set 1; S2 – Set 2; S3 – Set 3; IC/m – Intensity Count per meter; MTPL; Multiple.

Table 1c Example Log 3 – Detailed Geotech Log

From (m)	To (m)	Rock Type	Intact Rock Strength			Fracture Frequency					Cemented Joints		Micro Fractures		
			Strong MPa	Weak MPa	% Weak	Tot	Nat	Fol	S1	S2	S3	Count	Fill Type	IC/m	Fill Type
158.32	161.32	Anorthositic norite	R5	–	–	2	2	–	2	–	–	2	SP	–	–
161.32	162.52	Anorthositic norite	R5	R3	91.66	MTPL	√	–	√	√	–	–	–	–	–
162.52	163.37	Anorthositic norite & Websterite @ 162.97	R5	R3	50.59	5	5	–	3	2	–	3	SP	–	–
163.37	164.32	Websterite	R4	–	–	4	4	–	3	1	–	4	SP	–	–
164.32	165.84	Websterite	R4	–	–	3	3	–	3	–	–	3	SP	–	–
165.84	167.32	Websterite	R4	–	–	3	3	–	3	–	–	3	SP	–	–
167.32	169.29	Websterite	R4	R3	17.26	MTPL	√	–	√	√	–	2	SP	–	–
169.29	170.32	Websterite	R4	–	–	3	3	–	3	–	–	3	SP	–	–
170.32	171.23	Websterite	R4	R3	64.84	MTPL	√	–	√	√	–	7	SP	–	–
171.23	173.32	Websterite & Bronzite @ 172.12	R4	–	–	6	6	–	6	–	–	6	SP	–	–
173.32	175.34	Bronzite	R4	R3	12.87	MTPL	√	–	√	√	–	6	SP	–	–
175.34	176.32	Bronzite	R4	–	–	2	2	–	2	–	–	2	SP	–	–
176.32	178.14	Bronzite	R4	R0	17.58	3	3	–	3	–	–	3	SP	–	–

A wealth of insightful geotechnical information was obtained from the careful examination of the drilling campaign core. The distribution of RMR values from the sampled locations is shown in Figure 3. From the cumulative frequency distribution, it can be noted that 25% of the sampled locations are below an RMR value of 69.5 while 50% are below 75.5, calling for the need to carefully demarcate the deposit into appropriate zones for pillar and support design.

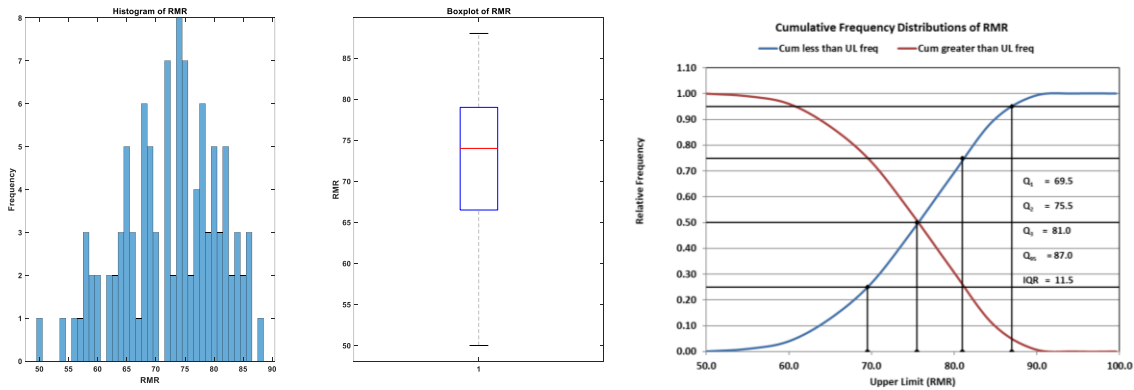


Fig. 3 RMR distribution at sampled locations: histogram, boxplot, and cumulative frequency.

2.2 Simple kriging background

Kriging is a geostatistical interpolation technique named after Danie Krige, a South African engineer who pioneered the method in the mining industry (Oliver and Webster, 2015; Bostan, 2017; Nhut, 2023). It is used to predict unknown values of a variable across a region from a scattered set of observed values. The method is grounded in the theory of regionalised variables, which posits that spatial phenomena can be modelled as realisations of random processes (Sen and Sen, 2009). Kriging not only estimates the value at unsampled locations but also provides a measure of estimation uncertainty. Simple kriging is a foundational geostatistical method used for spatial interpolation, where the goal is to predict the value of a regionalised variable at unsampled locations based on observations from sampled locations. The method relies on the assumption of stationarity, specifically that the mean and variance of the regionalised variable are constant across the area of interest (Boumpoulis et al, 2023). This underlying assumption distinguishes simple kriging from other Kriging methods that may allow for varying means (as in Universal Kriging) or other more complex models of spatial variation. The fundamental concepts of simple kriging are discussed in the following section.

2.2.1 Regionalised variable theory, stationarity assumption, and covariance and variogram

The regionalised variable theory postulates that spatially distributed variables (e.g., mineral concentrations, and soil properties) can be modelled as both deterministic and random. These variables, when observed at specific locations, are known as "regionalised variables." In simple kriging, the process is assumed to be stationary, meaning the statistical properties (mean, variance) of the regionalised variable do not change over space. This implies a constant mean across the entire study area and a covariance function that depends only on the distance and direction between locations, not on their absolute positions. The spatial dependency between the values of a regionalised variable at different locations is described by the covariance function or its counterpart, the variogram. The variogram is a function of the distance between two locations and describes how variance changes with distance.

2.3 Variogram modelling

The spatial variability and correlation structure of the sampled RMR values were characterised using variogram analysis. The experimental variogram $\gamma(h)$ is defined by Equation 1.

$$\gamma(h) = \frac{1}{2N(h)} \sum_{i=1}^{N(h)} [Z(x_i) - Z(x_i + h)]^2 \quad (1)$$

Where h is the lag distance
 $N(h)$ is the number of data pairs at lag h
 $Z(x_i)$ are the observed RMR values at locations x_i

Theoretical variogram models (Spherical, Gaussian, and Exponential models), see Figure 4 and Table 2, were fitted to the experimental variogram following the procedure described by Zvarivadza (2023). This facilitates the spatial structure characterisation of RMR across the deposit.

2.4 Simple kriging estimation

Simple kriging was employed to estimate the geotechnical parameter RMR at unsampled locations. The simple kriging estimator $\hat{Z}(x_0)$ at location x_0 is given by Equation 2.

$$\hat{Z}(x_0) = m + \sum_{i=1}^n \lambda_i [Z(x_i) - m] \quad (2)$$

Where m is the known global mean of the dataset
 λ_i are the kriging weights
 $Z(x_i)$ are the observed RMR values at locations x_i
 n is the number of neighbouring data points used in the estimation

The kriging weights λ_i are determined by solving the kriging system, Equation 3.

$$\sum_{j=1}^n \lambda_j \gamma(x_i - x_j) = \gamma(x_i - x_0), \sum_{j=1}^n \lambda_j = 1, \forall i = 1, 2, \dots, n \quad (3)$$

Note that in simple kriging, the constraint of weights adding to 1 is not required because the mean m is assumed to be known and constant throughout the domain.

2.5 Cross-validation

A cross-validation exercise was carried out to assess the performance of the semi-variogram models fitted to the experimental variogram. Nine performance metrics were determined for each fitted model semi-variogram i.e. Mean Squared Error (MSE), Mean Absolute Error (MAE), Root Mean Squared Error (RMSE), Mean Absolute Percentage Error (MAPE), Median Absolute Error (Median AE), R-squared (R^2), Correlation Coefficient (Corr Coeff), Explained Variance (EV), and Standard Deviation of Residuals (Std Dev R).

3 Results

3.1 Variogram analysis

The results of the Variogram analysis are presented in Figure 4 and Table 2. Note that C_0 is the nugget effect; C_T is the total sill; C_1 is the Spherical component, that is $C_T - C_0$.

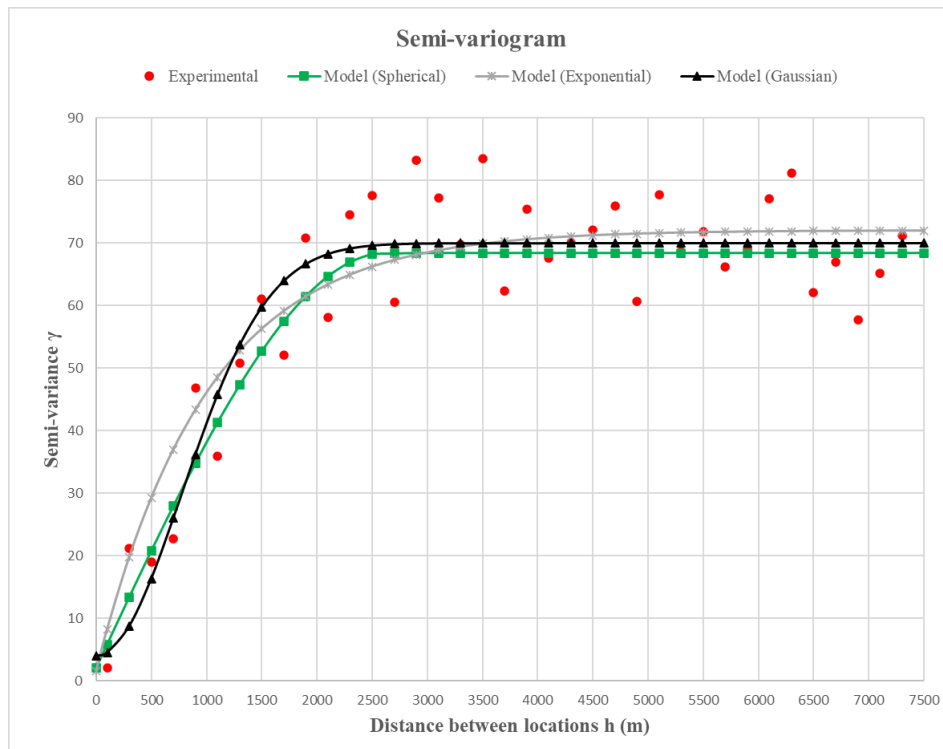


Fig. 4 Experimental semi-variogram and fitted model semi-variograms

Table 2 Fitted model semi-variograms and the values of their parameters

Spherical Model Semi-variogram	Gaussian Model Semi-variogram	Exponential Model Semi-variogram
$\gamma(0) = 0$ $\gamma(h) = C_0 + C_1 \left(\frac{3h}{2a} - \frac{1h^3}{2a^3} \right)$ for $0 < h < a$ $\gamma(0) = C_0 + C_1$ for $h > a$	$\gamma(0) = 0$ $\gamma(h) = C_0 + C_1 \left[1 - \exp \left(-\frac{h^2}{a^2} \right) \right]$ for $h > 0$	$\gamma(0) = 0$ $\gamma(h) = C_0 + C_1 \left[1 - \exp \left(-\frac{h}{a} \right) \right]$ for $h > 0$
$C_0: 2.0; C_T: 68.4; C_1: 66.4; a: 2627$	$C_0: 4.0; C_T: 70; C_1: 66; a: 1100$	$C_0: 1.5; C_T: 72; C_1: 70.5; a: 1000$

3.2 Cross-validation results

The cross-validation performance metrics (see Table 3) for the Spherical, Gaussian, and Exponential variogram models in estimating Rock Mass Rating (RMR) and delineating geotechnical zones in the Great Dyke deposit reveal key observations about model suitability and accuracy.

Table 3 Cross-validation performance metrics

Performance Metric	Spherical Model	Gaussian Model	Exponential Model
Mean Squared Error (MSE)	30.4571	77.8482	82.1797
Mean Absolute Error (MAE)	5.1165	8.0951	7.4720
Root Mean Squared Error (RMSE)	5.5188	8.8232	9.0653
Mean Absolute Percentage Error (MAPE) (%)	11.8715	18.9000	25.4887
Median Absolute Error (Median AE)	5.2101	7.5333	6.7249
R-squared (R^2)	0.9270	0.8289	0.8270
Correlation Coefficient (Corr Coeff)	0.9949	0.9866	0.9518
Explained Variance (EV)	0.9898	0.9729	0.9029
Standard Deviation of Residuals (Std Dev R)	2.0686	3.5097	6.7915

Among the three models, the spherical model demonstrates the highest performance with an MSE of 30.46, MAE of 5.12, and RMSE of 5.52. These lower error metrics indicate that the spherical model provides more accurate predictions of RMR values, with minimal deviation from observed data. The MAPE for the spherical model is 11.87%, significantly lower than the 18.90% for the Gaussian model and the 25.49% for the exponential model, further emphasising the superior fit of the spherical model. The R^2 value of 0.93 and a Corr Coeff of 0.995 also confirm that the spherical model has a strong positive correlation with the observed data, making it highly reliable for spatial estimation.

The exponential model has the lowest performance metrics, with an MSE of 82.18, RMSE of 9.07, and MAPE of 25.49%. These values suggest a higher level of prediction error, indicating that the exponential model may not capture the spatial variability of RMR as effectively. Although the exponential model has an R^2 value of 0.83 and a Corr Coeff of 0.952, these metrics are lower than those of the spherical and Gaussian models, reflecting its comparatively weaker predictive power for this application. The Gaussian model offers a middle ground between the spherical and exponential models, with an MSE of 77.85 and an RMSE of 8.82. While its R^2 value (0.83) and Corr Coeff (0.987) are comparable to those of the spherical model, the performance of the Gaussian model is slightly weaker, as indicated by its higher MAE and MAPE values. All in all, the cross-validation results suggest that the spherical model is the most appropriate for estimating RMR and defining geotechnical zones in the studied Great Dyke deposit. Its lower error metrics and higher correlation with observed data make it a more reasonable choice, providing reliable spatial predictions essential for accurate geotechnical characterisation and safer pillar design.

3.3 Geotechnical zoning

Based on the simple kriging estimates, the deposit was delineated into distinct geotechnical zones. Zone boundaries were defined where significant changes in geotechnical parameters occurred, facilitating tailored design approaches for each zone. The deposit was designated into three main zones: Geotechnical Zone 1 (GZ1), Geotechnical Zone 2 (GZ2), Geotechnical Zone 3 (GZ3 – divided into South West Zone (GZ3-SW) and South East Zone (GZ3-SE)). The geotechnical zones are demarcated in Figure 5 and the RMR ranges are shown in Table 4.

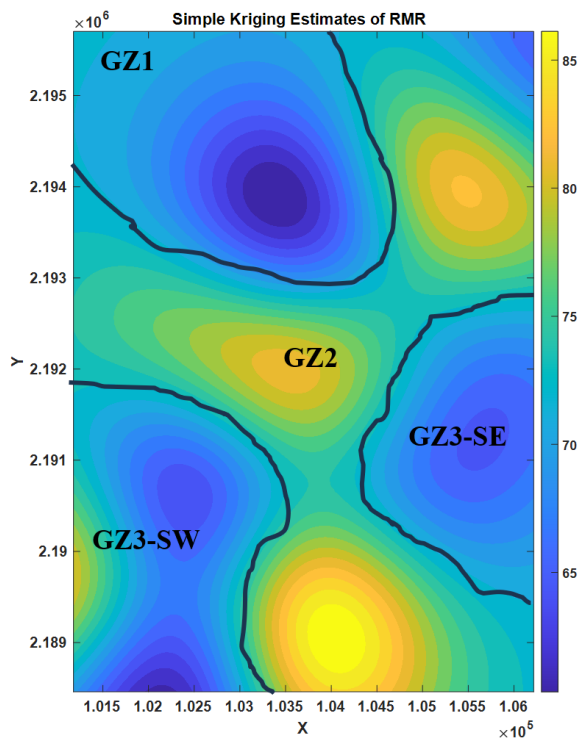


Table 4 Geotechnical zones from simple kriging

Geotechnical zone	RMR range	Comment
GZ1	60 - 72	Characterised by relatively lower RMR values.
GZ2	74 - 87	Exhibits higher RMR values.
GZ3-SW	61 - 73	Display relatively lower RMR values than GZ2. Small portion is similar to GZ2
GZ3-SE	65 - 73	Display relatively lower RMR values than GZ2

Fig. 5 Simple kriging estimates and geotechnical zones

3.3.1 Geotechnical Zone 1

GZ1 is characterised by relatively lower RMR values compared to other zones, as indicated by the darker blue contours. Lower RMR values reflect reduced rockmass quality, often due to factors such as increased joint frequency, poor rock integrity, or the presence of faulting and fracturing. This indicates that GZ1 traverses several geological structures which weaken the rockmass. From a pillar design perspective, the lower RMR values in GZ1 indicate that larger or more strong pillars may be required to provide adequate support. As an alternative, additional reinforcement measures, such as rock bolting or grouting, could be necessary to enhance the stability of pillars in this zone. Mining practitioners can implement tailored pillar designs that account for the specific geotechnical challenges present in this area by understanding the unique characteristics of GZ1, thereby reducing the risk of failure and improving mine safety.

3.3.2 Geotechnical Zone 2

GZ2 exhibits higher RMR values, represented by the yellow-green contours. This zone has a more competent rockmass with fewer geological structures and stronger rock quality. High RMR values indicate a rockmass that can withstand greater loads, providing more support for mining operations and reducing the risk of failure. The higher RMR values of GZ2 show that smaller pillars are feasible without compromising stability, maximising ore recovery from this area. The high RMR values also reduce the need for additional reinforcement, making this zone economically advantageous for mining operations. It remains essential, however, to monitor any localised structural anomalies within GZ2 to ensure that these favourable conditions are consistent throughout the zone.

3.3.3 Geotechnical Zone 3

GZ3 is subdivided into the South West Zone (GZ3-SW) and South East Zone (GZ3-SE) based on spatial RMR variations and physical locations of these portions of the deposit. Both sub-zones display relatively lower RMR values than GZ2. GZ3 is characterised by moderately low RMR values, suggesting a weaker rockmass than GZ2 but slightly more competent than GZ1. This implies a need for intermediate pillar sizes or reinforcements that are more substantial than those required for GZ2 but potentially less extensive than those in GZ1.

4 Discussion

The application of simple kriging provided a useful method for estimating geotechnical parameters. The technique proves critical for accurately estimating Rock Mass Rating (RMR) values across spatially variable rockmasses, especially in a complex geological setting like the Great Dyke. Simple kriging enables the interpolation of RMR values between drill holes, overcoming the limitations posed

by widely spaced boreholes. This spatial estimation approach provides a clearer understanding of the rockmass quality, allowing for the delineation of distinct geotechnical zones based on RMR values. The identified geotechnical zones (GZ1, GZ2, GZ3-SW, and GZ3-SE) reflect variations in rock quality, with each zone demanding specific pillar design and support strategies to ensure mine stability and safety. GZ1 and GZ3, with lower RMR values, for example, are characterised by weaker rockmasses, requiring larger pillars and additional reinforcement measures. GZ2, with higher RMR values, in contrast, shows stronger rock quality, where smaller pillars may suffice, optimising ore extraction. This targeted approach to pillar design based on geotechnical zoning not only improves safety but also enhances resource recovery, demonstrating the economic significance of the study. The importance of the study lies in its contribution to sustainable mining practices in the Great Dyke region. The study addresses spatial variability in rockmass properties by applying geostatistical techniques, which traditional empirical methods might overlook. The use of simple kriging for RMR estimation ensures more reliable spatial predictions, reducing the risk of pillar failure and promoting long-term stability. The research shows the value of geostatistics in rock engineering, offering a model for other complex ore deposits where spatial variability must be managed to balance safety, efficiency, and resource utilisation.

5 Conclusion

Applying simple kriging for geotechnical characterisation in the Zimbabwean Great Dyke provides a critical advancement in spatially predicting rockmass quality. This approach enables a clearer understanding of RMR variations across the deposit, allowing for more effective delineation of geotechnical zones. Through spatial interpolation, simple kriging addresses the limitations posed by widely spaced boreholes, creating reliable, continuous RMR estimates that traditional empirical methods cannot achieve. These detailed RMR distributions inform pillar design, ensuring that support structures are tailored to the specific rock quality of each zone. The practical implications of this research are profound. Mining operations can enhance both safety and economic efficiency by integrating simple kriging into geotechnical assessments. Geotechnical zones with lower RMR values, such as GZ1 and portions of GZ3, require larger or reinforced pillars, while high-RMR areas like GZ2 permit smaller pillars, optimising ore recovery. This zoning approach not only mitigates the risk of pillar failure but also supports sustainable resource utilisation. The study thus establishes a model for other mineral deposits with complex geology, where spatial variability must be managed to balance operational safety and profitability. The adoption of simple kriging represents a significant step toward more data-driven and resilient mining practices in the Great Dyke and similar deposits worldwide.

References

- Bostan, P., 2017. Basic kriging methods in geostatistics. *Yuzuncu Yil University Journal of Agricultural Sciences*, 27(1), pp.10-20.
- Boumpoulis, V., Michalopoulou, M. and Depountis, N., 2023. Comparison between different spatial interpolation methods for the development of sediment distribution maps in coastal areas. *Earth Science Informatics*, 16(3), pp.2069-2087.
- Chaumba, J.B., 2017. Hydrothermal alteration in the main sulfide zone at Unki Mine, Shurugwi Subchamber of the Great Dyke, Zimbabwe: Evidence from petrography and silicates mineral chemistry. *Minerals*, 7(7), p.127.
- Nhut, N.C., 2023. Kriging interpolation model: The problem of predicting the number of deaths due to COVID-19 over time in Vietnam. *EAI Endorsed Transactions on Context-aware Systems and Applications*, 9(1).
- Oliver, M.A. and Webster, R., 1986. Combining nested and linear sampling for determining the scale and form of spatial variation of regionalized variables. *Geographical analysis*, 18(3), pp.227-242.
- Sen, Z. and Sen, Z., 2009. Spatial Modeling. *Spatial Modeling Principles in Earth Sciences*, pp.203-269.
- Siachingoma, B., Hlatywayo, D.J., Midzi, V. and Mare, L., 2023. Geophysical mapping of the occurrence of platinum group elements in the main sulphide zone of the Great Dyke in Zimbabwe. *Journal of African Earth Sciences*, 202, p.104857.
- Wilson, A.H. and Prendergast, M.D., 1989. The Great Dyke of Zimbabwe: I-tectonic setting, stratigraphy, petrology, structure, emplacement and crystallisation. In *Magmatic sulphides field conference, Zimbabwe*. 5 (pp. 1-20).
- Zvarivadza, T., 2023. A conceptual study on the prediction of destress blasting efficiency using geostatistical approaches. In *ISRM 15th International Congress on Rock Mechanics and Rock Engineering & 72nd Geomechanics Colloquium-Challenges in Rock Mechanics and Rock Engineering* (pp. 487-492).